AIP | Applied Physics Letters

Tissue Doppler optical coherence elastography for real time strain rate and strain mapping of soft tissue

Ruikang K. Wang, Zhenhe Ma, and Sean J. Kirkpatrick

Citation: Appl. Phys. Lett. **89**, 144103 (2006); doi: 10.1063/1.2357854
View online: http://dx.doi.org/10.1063/1.2357854
View Table of Contents: http://apl.aip.org/resource/1/APPLAB/v89/i14
Published by the American Institute of Physics.

Tissue Doppler optical coherence elastography for real time strain rate and strain mapping of soft tissue

Ruikang K. Wang,[a] Zhenhe Ma, and Sean J. Kirkpatrick
Department of Biomedical Engineering, Oregon Health and Science University, Beaverton, Oregon 97006

(Received 15 June 2006; accepted 9 August 2006; published online 4 October 2006)

The authors present a tissue Doppler optical coherence elastography (tDOCE) method to image tissue movements, strain rates, and strains of soft tissue in real time. The method exploits the Doppler effect in optical coherence interferograms induced by tissue motion and measures the phase changes between successive A scans to resolve the instantaneous tissue displacement. The tDOCE system is capable of displaying the strain rates and strain maps of tissue subjected to a dynamic compression in real time. The system is demonstrated by the use of a heterogeneous tissue phantom with known mechanical properties. © *2006 American Institute of Physics*.
[DOI: 10.1063/1.2357854]

Optical coherence tomography (OCT) has been used to study the microscopic deformation of biological tissue under compressive stress,[1] which was later termed optical coherence elastography (OCE). The approach was based on a two-dimensional (2-D) image cross-correlation technique to track the speckle motion between successive OCT frames (B scan) obtained from tissue subjected to a quasistatic compression. There has seen successful application of this OCT imaging mode to characterize the evolution of biomechanical properties of developing engineered tissue.[2] The basic assumption for these previous embodiments is that the speckle in the OCT image is stable between successive B scans, which limits this technique to relatively small compressions between the B scans, normally less than the coherence length of the light source used. However, relatively large tissue movement rapidly decorrelates the speckle from one frame to another. In addition, tracking the speckle movement, thus the displacement of tissue, was accomplished by a search of the cross-correlation peaks between two moving windows over the entire OCT images. This is a time consuming procedure, making the real time online measurement difficult. Here we present an alternative approach, called tissue Doppler OCE (tDOCE) to visualize and quantify in real time the movements or displacements, and thus the strains and strain rates of tissue.

OCT is extremely sensitive to any particle movement in the sample, creating a Doppler effect in the resulting interference signal. This phenomenon was first utilized in time-domain OCT[3] (TdOCT) and later in frequency-domain (FdOCT) systems[4] to accurately measure fluid flow, including blood flow. Clearly, because of light scattering from tissue, any tissue movement also induces the Doppler effect in the interference signals. This feature has not been exploited in the OCT community. Our tDOCE system was developed based on the measurement of Doppler frequency shift induced by the instantaneous tissue motion; consequently the local displacement, strain rate, and strain can be accurately quantified and mapped in real time. Because FdOCT has inherent advantages over TdOCT in terms of imaging speed, detection sensitivity, and phase stability,[5] we will describe and demonstrate tDOCE as implemented with a spectral FdOCT system in this letter.

In spectral domain OCT, the interference signal between the reference light and the scattering light from within a sample is spectrally resolved by a linear array detector which is then Fourier transformed to obtain the amplitudes and phases of the light reflected from the sample as a function of depth. The amplitudes are used to generate the OCT structural images, whereas the phases are generally random, but fixed in position when the biological sample is static. However, a translation of the sample at the time t by an instantaneous distance $\Delta d(t)$ during the time interval τ between two successive A scans will induce a change in the measured phase of the reflected light given by $\Delta\phi(z,t)=2n\bar{k}\Delta d(t)$, where n is the refractive index of the sample and $\bar{k}$ is the average wave number. Calculating this phase difference at each depth z yields depth-resolved measurements of both the magnitude and direction of the axial displacement of tissue at the time t, i.e., $\Delta d(z,t)=\Delta\phi(z,t)\bar{\lambda}(4\pi n)^{-1}$. Similar to the phase-resolved optical Doppler tomography (PRODT) where the concern is the flow velocity,[3,4] the depth-resolved tissue velocity $v(z,t)$ in the beam direction can be obtained by $v(z,t)=\Delta\phi(z,t)\bar{\lambda}(4\pi n\tau)^{-1}$. After the depth-resolved instantaneous displacement and velocity are obtained, the strain rate map $\varepsilon'(z,t)$ can be generated and color coded to represent the local elastic properties of tissue,

$$\varepsilon'(z,t)=\frac{v(z,t)}{z_0}=\frac{\Delta\phi(z,t)\bar{\lambda}}{4\pi n\tau z_0}, \tag{1}$$

where z_0 is the initial depth of the sample before the compression. As a consequence, the depth-resolved displacement $d(z)$ and strain $\varepsilon(z)$ maps of the sample over the time duration T can be generated:

$$d(z)=\int_0^T \Delta d(z,t)dt=\int_0^T \frac{\Delta\phi(z,t)\bar{\lambda}}{4\pi n}dt, \tag{2}$$

$$\varepsilon(z)=\int_0^T \varepsilon'(z,t)dt=\int_0^T \frac{\Delta\phi(z,t)\bar{\lambda}}{4\pi n\tau z_0}dt. \tag{3}$$

Unlike the OCE previously developed where maintaining correlated speckle between successive OCT B scans restricts

[a]Author to whom correspondence should be addressed; electronic mial: r.k.wang@bme.ogi.edu

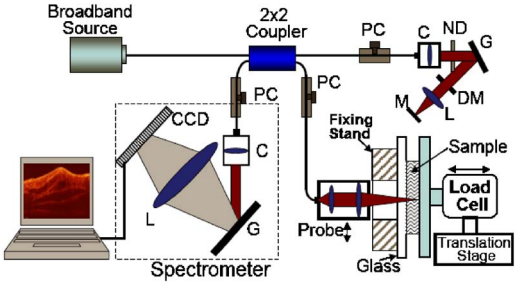

FIG. 1. (Color online) Schematic of the tDOCE system used in this study, where PC represents the polarization controller, C the collimator, ND the neutral density filter, DM the double pass mirror, L the lens, M the mirror, and G the grating.

its ability to obtain strain maps of tissue in real time, the current approach only requires that the speckle between the successive A scans be correlated. The calculations of tissue motion and strain maps are straightforward.

The schematic of the tDOCE system used in this study is shown in Fig. 1 that includes two main parts, one of which consisted of the spectral domain OCT system and the other the loading rig that was used to apply a dynamic force to compress the tissue. The OCT system has been described in detail previously.[6] Briefly, it used a light source with central wavelength of 842 nm and had the measured axial and lateral resolutions of 8 and 20 μm, respectively. The spectrometer had a designed imaging depth of 3.2 mm in air, capable of 29.2 kHz line rate. The B scan OCT image consisting of 500 A scans, corresponding to 2.5 mm, was obtained by lateral scanning of the probe controlled by the X scanner. The A-scan interval was 5 μm ensuring that the speckle in the interferograms was correlated between successive A scans, because the probing beam spot was 20 μm (transverse resolution). Imaging rate was set at 20 fps (frames per second) with τ=100 μs in this study.

The loading fixture cell consisted of a calibrated load cell mounted on a precision motorized translation stage that was used to compress the sample. Both the signals from the load cell representing the force applied and the translation stage indicating the actual displacement of the sample were measured for later comparison of the OCT measurements. A transparent glass slide (with a thickness of ~1.5 mm) was glued to a fixed stand that had a clear hole of 1 cm diameter in the middle that allowed the OCT probe beam to pass through freely. A triangular wave form of the movement was applied repeatedly to the sample with a magnitude of 400 μm and velocity of 400 μm/s in this study. At this slow rate of compression and assuming that the biological sample is nearly incompressible (i.e., Poisson's ratio ~0.5), the behavior of mechanical properties of tissue can be approximated as those in the quasistatic compression cases.[7] To demonstrate the tDOCE system, we used a tissue phantom made of 80% w/w poly(vinyl) alcohol (PVA) because the mechanical properties of this material are predictable if subjected to repeated freezing-thawing cycles.[8] A bilayer tissue phantom was made from PVA for this investigation with the top layer of thickness ~250 μm subjected to 7 freeze/thaw cycles and the bottom layer about 2.5 mm thickness subjected to 5 cycles. Based on prior mechanical testing in our laboratory, the expected ratio of dynamic stiffness was on the order of 1.5:1 between the two layers.

The bilayer phantom was preloaded with a stress of $\sim 2.94 \times 10^4$ N/m^2. The original thickness of the phantom at

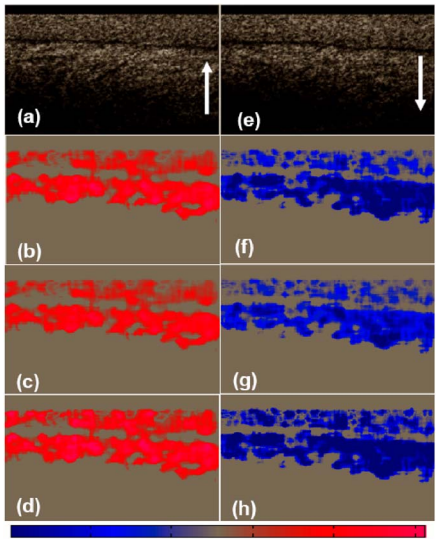

FIG. 2. (Color online) From top to bottom, OCT structural image, velocity, instantaneous displacement, and strain rate maps of the bilayer phantom during loading (left column) at t=0.5 s and unloading at t=1.5 s (right column), respectively. The color bar at the bottom was used to code the images other than (a) and (e) with the range from −120 to 120 μm for (b) and (f), from −12 to 12 nm for (c) and (g), and from −0.25 to 0.25 s^{-1} for (d) and (h), respectively. The arrows indicate the loading directions.

time t=0 was measured as ~2 mm. The sample was then compressed repeatedly as described above for 8 cycles (16 s) and then allowed rest for 5 s, during which time the OCT system continuously generated in real time the velocity, instantaneous displacement, and strain rate maps of the phantom. Figure 2 illustrates typical examples of the real time OCT image, velocity, instant displacement, and strain rate maps at t=0.5 s when the sample was being loaded [Figs. 2(a)–2(d)], and at t=1.5 s during unloading [Figs. 2(e)–2(h)], respectively. The physical size of the images shown is 1.2 $\times$ 2.5 mm^2 (depth $\times$ width). As was expected, the values of the velocity, instantaneous displacement, and strain rate maps of the tissue phantom change sign when the load was applied to the sample (positive, left column of Fig. 2), as compared to when the load was released (negative, right column of Fig. 2). More importantly, from Figs. 2(b)–2(d) and Figs. 2(f)–2(h), it can be seen that the absolute values in the top layer are less than those in the bottom layer, indicating that the top layer of the phantom is stiffer than that of the bottom layer, which was expected based upon prior mechanical testing of similar phantom materials.

To further quantify the elastic properties of the bilayered phantom used in this study, we collapsed each B-scan velocity image and averaged them into a single A-scan velocity profile. This collapsed A scan velocity profile was then plotted as a function of time as the load was applied to the sample. Fig. 3(a) gives such time varying velocity map over a time duration of 21 s. It is clearly seen that the tissue velocity alternates its sign during the loading and unloading periods, and then it approaches zero when it is at rest. In addition, the velocity in the top layer is seen to be slower than that in the bottom layer. By applying Eqs. (1)–(3) to Fig. 3(a), the results can be obtained and color coded to generate the time varying strain rate [Fig. 3(b)], displacement [Fig. 3(c)], and strain [Fig. 3(d)] maps, respectively. Figures 4(a) and 4(b) show the plots for the representative displacements and strains against time at four different depths in the sample, respectively. These results were com-

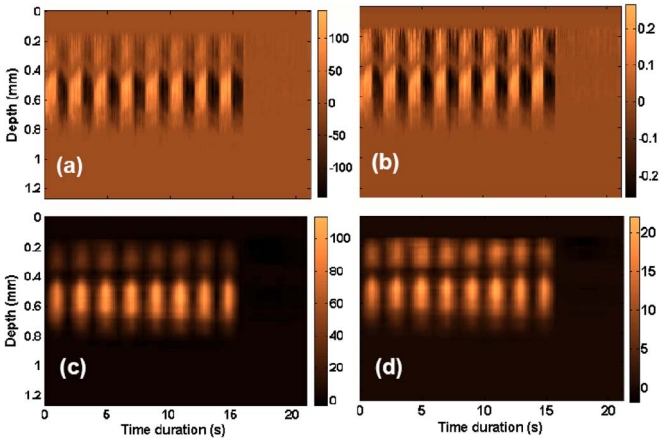

FIG. 3. (Color online) Integrated time varying (a) velocity (μm/s), (b) strain rate (s^{-1}), (c) displacement (μm), and (d) strain (%) maps, respectively, of the tissue phantom subjected to 8 loading cycles and then followed by a 5 s rest period.

pared with the actual displacement at $z=0.58$ mm and force measured online from the outputs of the translation stage and the load cell, respectively, synchronized with the OCT measurements. From Fig. 4(a), the time varying displacement of the sample during the loading and unloading cycles approximates well the triangular wave form at all the depths with the softer bottom layer displacing to a greater extent whereas the stiffer top layer displaced less. Further convincing evidence for the tDOCE measurement is from Fig. 4(b) where it is seen that the strains measured at the different depths are almost equal within each layer, indicating that the stiffness of the sample is the same if characterized separately for each layer. From this plot, the averaged ratio of the strains of the bottom layer to the top layer was calculated as $1.65\pm0.10:1$ that agreed well with the expected value of 1.5:1 as measured by a separate mechanical testing in our laboratory.

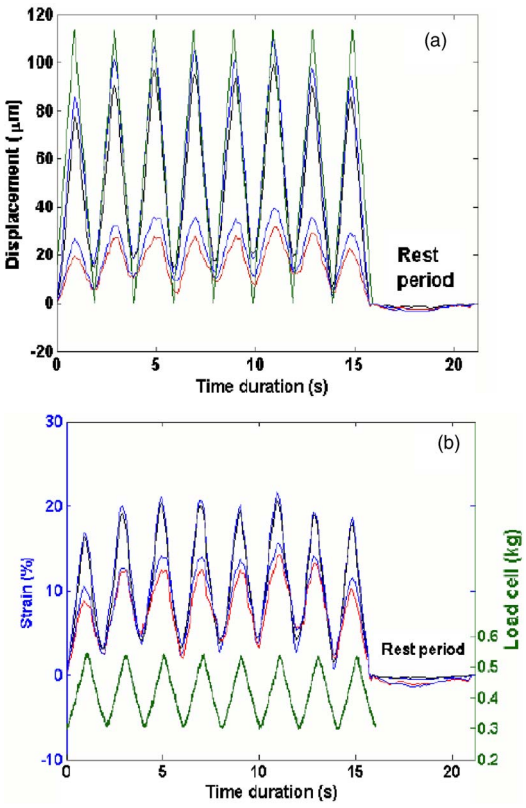

FIG. 4. (Color online) (a) Displacement and (b) strain profiles plotted against the time compared with the synchronized separate measurements of actual displacement [top curve in (a)] and force [bottom curve in (b)] applied to the phantom, respectively. The remainder of the curves from the bottom to the top represents the depth profiles at $z=0.26$, 0.29, 0.51, and 0.55 mm, respectively.

Like PRODT to measure flow velocity,[4,9] the accuracy and sensitivity of the tDOCE system to provide the elastic imaging of tissue are fundamentally limited by the phase sensitivity of the optical system. It has been shown that the noise in the measured phase changes between successive A scans is inversely proportional to the signal-to-noise ratio (SNR) of the system.[9] With typical OCT signals from biological tissues having SNRs ~50 dB, the measuring accuracy of phase changes induced by the tissue motion is ultimately limited to ~3 mrad. This suggests that the minimum resolvable displacement in tissue is ~0.15 nm for the current system with $\bar{\lambda}=840$ nm and $n=1.3$. Accordingly, the minimum resolvable tissue velocity and strain rate for the current system are approximately 4.4 μm/s and 0.44%/s with $\tau=34.1$ μs (29.2 kHz) and assuming the tissue thickness is 1 mm. The upper limit for the tDOCE to measure the tissue velocity and displacement is limited by the wrapping of phase changes between the successive A scans because all complex numbers have unique phase only modulo 2π. This would only allow a maximum movement between successive A scans of ~0.32 μm or tissue velocity of ~9.5 mm/s for $n=1.3$ and $\tau=34.1$ μs for the current system. Exceeding this upper limit on motion would result in a characteristic ringing making determination of the elastic properties of tissue ambiguous. Nevertheless, such a sensitivity and dynamic range of the measurement would serve most of applications for the elastic imaging *in vivo*.

With the current intense research interests in measuring the *in vivo* elastic properties of the normal and pathological tissues, tDOCE has the potential to provide both qualitative and quantitative means for characterizing the biomechanical properties at the micrometer scale within *in vivo* highly scattering tissue in real time.

This work was funded in part by Grant No. 1R21CA103824-02 from the National Institutes of Health.

[1]J. M. Schmitt, Opt. Express **3**, 6 (1998).
[2]H. J. Ko, W. Tan, R. Stack, and S. A. Boppart, Tissue Eng. **12**, 63 (2006).
[3]Z. P. Chen, T. E. Milner, S. Srinivas, X. J. Wang, A. Malekafzali, M. J. van Gemert, and J. S. Nelson, Opt. Lett. **22**, 1119 (1997).
[4]B. R. White, M. C. Pierce, N. Nassif, B. Cense, B. H. Park, G. J. Tearney, B. E. Bouma, T. C. Chen, and J. F. de Boer, Opt. Express **11**, 3490 (2003).
[5]M. A. Choma, M. V. Sarunic, C. Yang, and J. Izzat, Opt. Express **11**, 2183 (2003).
[6]R. K. Wang and Z. H. Ma, Phys. Med. Biol. **51**, 3231 (2006).
[7]K. J. Parker, L. S. Taylor, and S. Gracewski, J. Acoust. Soc. Am. **117**, 2705 (2005).
[8]K. J. M. Surry, H. J. B. Austin, A. Fenster, and T. M. Peters, Phys. Med. Biol. **49**, 5529 (2004).
[9]B. J. Vakov, S. H. Yun, J. F. de Boer, G. J. Tearney, and B. E. Bouma, Opt. Express **14**, 5483 (2005).